Materials Transactions, JIM, Vol. 39, No. 1 (1998), pp. 203 to 210

Finite Difference Simulation of Peritectic Transformation in Iron-Carbon Alloy

Kiyotaka Matsuura and Masayuki Kudoh

Division of Materials Science and Engineering, Graduate School of Engineering, Hokkaido University, Kita-ku, Sapporo, Hokkaido 060-8628, Japan

The process of peritectic transformation during cooling of iron-carbon alloys has been simulated by a numerical analysis based on the direct finite difference method. During the peritectic transformation, austenite is produced from δ-ferrite by precipitation and from liquid by crystallization. The amount of precipitated austenite is approximately four times as large as that of the crystallized one. Both the amounts of the precipitated austenite and the crystallized one increase when the carbon content of the alloy increases from 0.09 to 0.17 mass%, but they decrease when it increases from 0.17 to 0.53 mass%. The finishing temperature of the peritectic transformation falls with the increase in carbon content from 0.09 to 0.17 mass%, but it rises with the further increase in carbon content to 0.53 mass%. The increase in cooling rate accelerates the transformation rate and reduces the finishing temperature.

(Received June 2, 1997)

Keywords: *peritectic reaction, δ/γ transformation, solidification, diffusion, computer simulation, iron-carbon system, carbon steel*

I. Introduction

When a molten steel with a carbon content between 0.09 and 0.53 mass% is cooled, δ-ferrite crystallizes from the liquid as the primary crystal at a liquidus temperature, and then the primary crystal and the residual liquid react at a peritectic temperature of 1768 K to transform into the secondary crystal of austenite, according to an iron-carbon binary equilibrium phase diagram[1] depicted in Fig. 1. This phenomenon is referred to as peritectic transformation or peritectic reaction and is described as $\delta+L\rightarrow\gamma$, where δ, L and γ are δ-ferrite, liquid and austenite, respectively. Because austenite has significantly different physical properties from those of δ-ferrite, the peritectic transformation leads to some undesirable phenomena such as generation of tensile stress[2], segregation of alloying elements[3], precipitation of inclusions[4], and so on. Particularly, generation of tensile stress is remarkably harmful, because it causes cracking on the surface of continuously cast slabs[5]. For optimum control of these phenomena, the rate of peritectic transformation is considered to be an important guide. When the transformation proceeds slowly, for instance, the generated stress is considered not to increase to a level high enough for surface cracking to occur, because the stress may be relaxed by creep deformation during a long period of transformation. Similarly, segregation of alloying elements is expected to be reduced by diffusion. Thus, the rate of peritectic transformation can significantly influence the quality of cast slabs of carbon steel.

Chuang *et al.*[6] calculated the rate of peritectic transformation during cooling of an iron-carbon alloy containing 0.39 mass% carbon, and showed that the temperature drop during peritectic transformation varied from 2.6 to 4.4 K, when the dendrite spacing varied from 301.6 to 29.5 μm depending on the local solidification time ranging from 388 to 1 s. However, they presented the result for only one carbon content. Fredriksson and Stjerndahl[7] made a new calculation with a very simple analytical model, and showed that the temperature drop during peritectic transformation varied with carbon content of the alloy and with the solidification rate; the temperature drop reached the maximum at 0.17 mass% carbon, and the maximum value varied from 6.5 to 10.3 K, when the solidification rate varied from 0.5 to 5.0 mm/min. The calculation made by Chuang *et al.* and that by

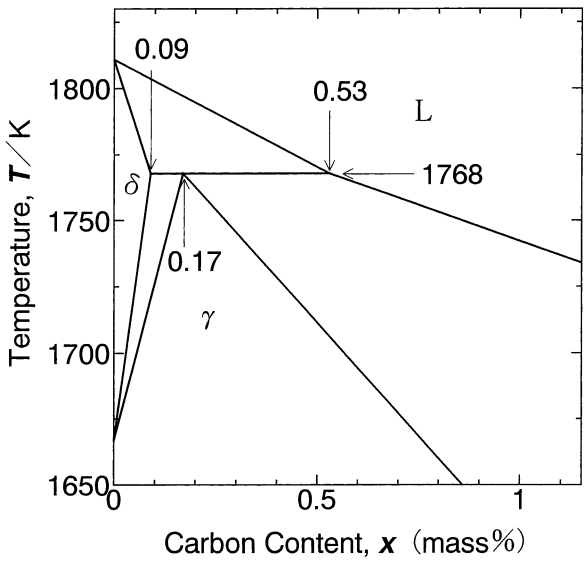

Fig. 1 An iron-carbon binary equilibrium phase diagram[1]. Symbols δ, γ and L are the abbreviations for δ-ferrite, austenite and liquid, respectively.

Fredriksson and Stjerndahl were both based on a diffusion-controlled growth mechanism: they assumed that austenite phase grew into both phases of δ-ferrite and liquid by diffusion of carbon from liquid through austenite into δ-ferrite, and that the rate-determining step of the growth was the diffusion of carbon in austenite, because the diffusion coefficient of carbon is the smallest in austenite. Both the research groups calculated the positions of the moving interfaces from the mass balance across the interfaces, but the mass balance equations were different between them. Chuang *et al.* expressed the mass balance equation taking account of the change in carbon concentration of the interfaces with temperature and solved it by using Green's function method, while Fredriksson and Stjerndahl considered only the mass balance of carbon at a temperature and obtained the relationship between the temperature drop and the thickness of austenite phase by integrating the mass balance equation. Enomoto[8] examined the validity of the additivity rule in non-isothermal diffusion-controlled growth of precipitates in steel, and found that when the solubility changes with temperature, adding of the results obtained from a diffusion equation formulated under an iso-thermal condition produces a systematic error. Therefore, the results obtained by Fredriksson and Stjerndahl may have included an error.

The present authors[9]-[12] have measured the growth rate of austenite phase during iso-thermal peritectic transformation and that during cooling at various cooling rates by means of a model experiment based on a solid/liquid diffusion couple method, and have found that the growth rate increases with cooling rate and that the increase in growth rate includes the precipitation of austenite phase from δ-ferrite phase and the crystallization of it from liquid phase during cooling. Our results support the results of Enomoto's examination. However, in our previous studies, we have not considered the change in dendrite size with cooling rate, because we performed model experiments using a diffusion couple with a very huge size compared with the actual dendrite size. In the present study, we simulate the process of the peritectic transformation during cooling of iron-carbon alloys by the numerical analysis taking account of the change in dendrite size with cooling rate and the precipitation and crystallization of austenite during cooling, and investigate the effects of carbon content and cooling rate on the rate of peritectic transformation.

II. Procedure

1. Modelling of peritectic transformation

Figure 2 schematically shows (a) a dendritic structure of a solidifying carbon steel and the profile of temperature in the solidification direction, and (b) the distribution of carbon concentration in the volume element considered in this calculation. The morphology of the dendrites was taken to consist of parallel plates, as proposed by Brody and Flemings[13]. The distance between the

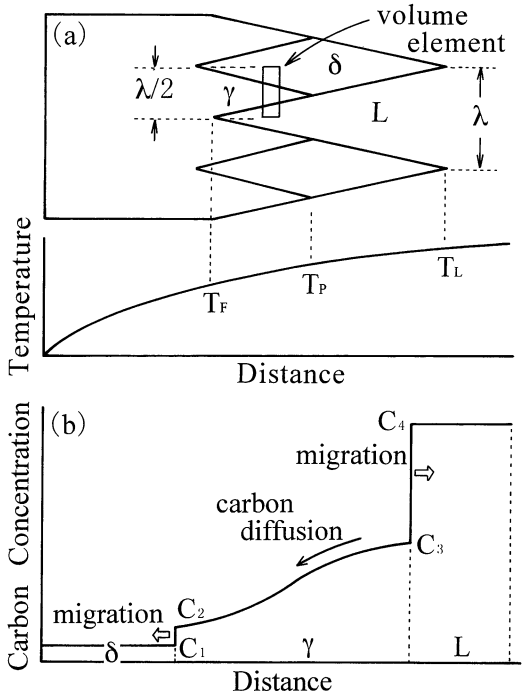

Fig. 2 (a) a dendritic structure and the profile of temperature near the mold wall and (b) the distribution of carbon concentration in the volume element considered in this calculation. Symbols T_L, T_P and T_F are the abbreviations for the liquidus temperature, peritectic temperature and finishing temperature of the peritectic transformation, respectively.

dendrites, λ (μm), was calculated from the cooling rate, v (K/s), by using eq. (1)[14].

$$\lambda = 2640(60v)^{-0.48} \quad (1)$$

The peritectic transformation starts at the peritectic temperature of T_P, and austenite phase is produced at δ-ferrite/liquid interface. Under an equilibrium condition, the starting and finishing temperatures of the peritectic transformation are both T_P. Under a condition of cooling at a finite cooling rate, however, the transformation does not finish at T_P, and therefore, below T_P, an envelope structure which consists of the three phases of δ-ferrite, austenite and liquid is developed, as illustrated in Fig. 2. According to the diffusion-controlled growth mechanism of the peritectic transformation, an austenite phase grows by diffusion of carbon through austenite. Because of a finite time for diffusion, the peritectic transformation continues to a temperature of T_F, at which the envelope structure disappears.

In our model of the peritectic transformation, during cooling from T_P, the austenite phase grows by precipitation from the δ-ferrite phase and crystallization from the liquid phase, in addition to the diffusional growth based on the diffusion-controlled growth mechanism. We simulated a continuous cooling at a rate of v(K/s) as repeating of the sequence of isothermal holding and quenching at a very small step in time, Δt(s), and temperature, ΔT(K). The cooling rate is expressed in eq. (2).

$$v=\Delta T\Delta t^{-1} \quad (2)$$

We made the following assumptions for this calculation.

(1) The growth of austenite phase proceeds by carbon diffusion during isothermal holding for Δt and by precipitation and crystallization during quenching by ΔT.

(2) Diffusion of carbon is complete in both phases of δ-ferrite and liquid.

(3) Both the precipitation and crystallization occur without undercooling.

(4) The sites of precipitation and crystallization are limited to δ-ferrite/austenite interface and austenite/liquid interface, respectively.

2. Growth of austenite by diffusion

We have previously investigated the growth rate of the austenite phase during isothermal peritectic transformation in iron-carbon system both experimentally[8][10] by using a solid/liquid diffusion couple method and theoretically[11] by using the diffusion-controlled growth mechanism, and have obtained the relationship between the holding temperature and the parabolic rate constant, which is the coefficient in the parabolic law described in eq. (3).

$$x=at^{1/2} \quad (3)$$

where x is the thickness of the austenite phase (μm), t is the holding time (s) and a is the parabolic rate constant (μm·s$^{-1/2}$). The parabolic rate constant for the migration of δ-ferrite/austenite interface, $a_{\delta/\gamma}$, and that for the migration of the austenite/liquid interface, $a_{\gamma/L}$, were approximated by eqs. (4) and (5), respectively[11]:

$$a_{\delta/\gamma}=4.27(D_\gamma\Delta C)^{1/2} \quad (4)$$

$$a_{\gamma/L}=0.86(D_\gamma\Delta C)^{1/2}. \quad (5)$$

where D_γ is the diffusion coefficient of carbon in the austenite phase and ΔC is the difference between the carbon concentration in the austenite phase at the δ-ferrite/austenite interface and that at the austenite/liquid interface, and they were expressed as a function of temperature in eqs. (6)[15] and (7)[1], respectively.

$$D_\gamma=0.761\times10^8\exp(-134400R^{-1}T^{-1}) \quad (\mu m^2\cdot s^{-1}) \quad (6)$$

$$\Delta C=-7.545\times10^{-3}T+13.34 \quad (\text{mass\%}) \quad (7)$$

where R is a gas constant (J K^{-1} mol^{-1}) and T is the temperature (K). As T goes down from T_P, ΔC increases from zero, while D_γ decreases. Because the increase in ΔC is more remarkable than the decrease in D_γ, both $a_{\delta/\gamma}$ and $a_{\gamma/L}$ increase with the decrease in temperature.

The increment in thickness of the austenite phase due to the diffusional growth during isothermal holding for Δt is given by eq. (8):

$$\Delta x_{Diff}=(dx/dt)\Delta t \quad (8)$$

where dx/dt is the migration velocity of the interface and is given in eq. (9), which was obtained by differentiating eq. (3):

$$dx/dt=a^2(2x)^{-1}. \quad (9)$$

Consequently, one can obtain the increment in thickness of the austenite phase due to the diffusional migration of the δ-ferrite/austenite interface and that due to the diffusional migration of the austenite/liquid interface, by using eqs. (10) and (11), respectively.

$$\Delta x_{Diff,\delta/\gamma}=a^2_{\delta/\gamma}(2x)^{-1}\Delta t \quad (10)$$

$$\Delta x_{Diff,\gamma/L}=a^2_{\gamma/L}(2x)^{-1}\Delta t \quad (11)$$

3. Growth of austenite by precipitation and crystallization

Figure 3 shows a schematic profile of carbon concentration over the three phases of δ-ferrite, austenite and liquid. Symbols C_1 and C_2 are the equilibrium carbon concentrations of δ-ferrite and austenite at the δ-ferrite/austenite interface, and C_3 and C_4 are those of austenite and liquid at the austenite/liquid interface. The values of C_1 through C_4 change with temperature, T, as shown in the equilibrium phase diagram depicted in Fig. 1. The relationships between C_1 through C_4 (mass%) and T (K) were approximated as eqs. (12) through (15).

$$C_1=8.91\times10^{-4}T-1.48 \quad (12)$$

$$C_2=1.68\times10^{-3}T-2.81 \quad (13)$$

$$C_3=-5.86\times10^{-3}T+10.53 \quad (14)$$

$$C_4=-1.83\times10^{-2}T+32.89 \quad (15)$$

As a result of quenching from T to $(T-\Delta T)$, the equilibrium carbon concentrations in δ-ferrite and austenite at the δ-ferrite/austenite interface decrease from C_1 and C_2 to C_1' and C_2', respectively, as illustrated in Fig. 3. Simultaneously, the equilibrium carbon concentrations in austenite and liquid at austenite/liquid interface increase from C_3 and C_4 to C_3' and C_4', respectively.

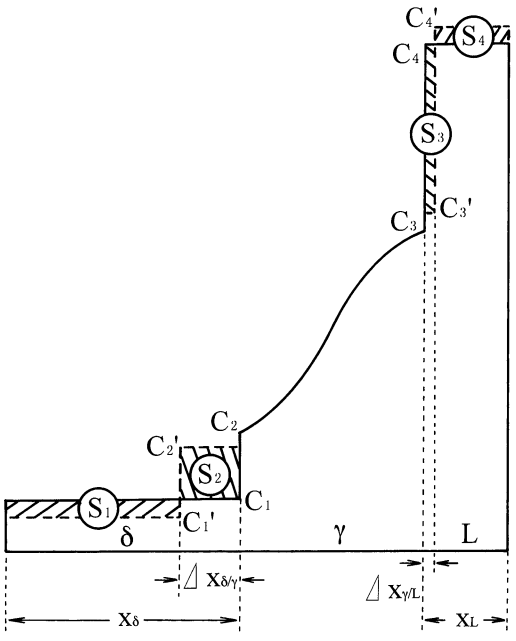

Fig. 3 Schematic profile of carbon concentrations over δ-ferrite, austenite and liquid phases.

Owing to the decrease in carbon concentration of the δ-ferrite phase from C_1 to C_1', the amount of carbon corresponding to the area symbolized as S_1 in Fig. 3 becomes excessive. This amount of carbon was assumed to be consumed by the precipitation of the austenite phase at the δ-ferrite/austenite interface, which corresponds to the area symbolized as S_2 in Fig. 3. Therefore, from the condition that $S_1=S_2$, the thickness of the austenite phase which precipitates on quenching from T to $(T-\Delta T)$ is expressed as eq. (16).

$$\Delta x_{\delta/\gamma}=x_\delta(C_1-C_1')/(C_2'-C_1') \tag{16}$$

where x_δ is the thickness of the δ-ferrite phase at T. Similarly, from the condition that $S_3=S_4$, the thickness of austenite phase which crystallizes at austenite/liquid interface on quenching from T to $(T-\Delta T)$ is expressed as eq. (17).

$$\Delta x_{\gamma/L}=x_L(C_4'-C_4)/(C_4'-C_3') \tag{17}$$

where x_L is the thickness of the liquid phase at T.

4. Conditions of calculation

The initial thickness of the δ-ferrite phase, $x_{\delta 0}$, and that of the liquid phase, x_{L0}, were calculated by using eqs. (18) and (19), respectively.

$$x_{\delta 0}=f_{\delta 0}\lambda/2 \tag{18}$$

$$x_{L0}=(1-f_{\delta 0})\lambda/2 \tag{19}$$

where $f_{\delta 0}$ is the initial fraction of δ-ferrite phase and was given as the function of carbon content based on the lever rule, while λ is the dendrite spacing and was evaluated from the cooling rate by using eq. (1). The cooling rate, v, was varied from 0.01 to 10 K/s. According to eq. (1), when v increases from 0.01 to 10 K/s, λ decreases from 3374 to 122 μm. The starting temperature of the peritectic transformation was taken as the equilibrium peritectic temperature of 1768 K, because undercooling was not considered. The temperature step, ΔT, was determined from v and Δt by using eq. (2). The time step, Δt, was varied during repetition of the calculation routines so that the increment in thickness of austenite phase per one step expressed in eq. (20) fell in a range between 0.01 and 0.1 μm.

$$\Delta x_\gamma=(\Delta x_{Diff,\delta/\gamma}+\Delta x_{Diff,\gamma/L})+(\Delta x_{\delta/\gamma}+\Delta x_{\gamma/L}) \tag{20}$$

The thickness of austenite phase at a time of t was calculated by using eq. (21), and the result was substituted into eqs. (10) and (11) to calculate the increment in thickness by diffusional growth during the next time step. This calculation was continued until either x_δ or x_L decreases to zero.

$$x|_{t=t}=x|_{t=t-\Delta t}+\Delta x_\gamma \tag{21}$$

III. Results and Discussion

1. Change in fraction of each phase during peritectic transformation

Figures 4 through 6 show the changes in fraction of the three phases of δ-ferrite, austenite and liquid during peritectic transformation in iron-carbon alloys with carbon content of 0.12, 0.17 and 0.25 mass%, which correspond to a hypo-peritectic composition, the peritectic composition and a hyper-peritectic composition, respectively. The effect of cooling rate is shown by varying it from 0.01 to 0.10 K/s. When the carbon content increases, the initial fraction of the δ-ferrite phase decreases, while that of the liquid phase increases. In the alloy with a hypo-peritectic composition, when the fraction of the liquid phase decreases to zero, the peritectic transformation finishes (see Fig. 4). On the other hand, in the alloy with a hyper-peritectic composition, when the fraction of the δ-ferrite phase decreases to zero, the peritectic transformation finishes (see Fig. 6). In the alloy with the peritectic composition, the fraction of δ-ferrite phase and that of liquid phase reach zero at the same time (see Fig. 5). In all the alloys, the decrease in the δ-ferrite phase is faster than that in the liquid phase, which is explained from the difference in height of the cliff in the concentration profile shown in Fig. 2(b); the high cliff at the austenite/liquid interface induces a large amount of outward flow of carbon from the liquid phase upon the slight migration of the austenite/liquid interface, while this amount of carbon is consumed in the large migration of the δ-ferrite/austenite interface because of the low cliff at the δ-ferrite/austenite interface. When the cooling rate is high, the change in each fraction is fast, which is caused by the faster diffusional growth at the lower temperatures as described in eqs. (4) through (7) and by faster precipitation and solidification at higher cooling rates.

Figure 7 shows the effect of carbon content on the growth rate of the austenite phase during peritectic transformation. The growth rate of the austenite phase increases with carbon content. This can be explained from the fraction of the liquid phase which increases with the carbon content, as follows. During cooling from the peritectic temperature, the austenite phase grows by precipitation from the δ-ferrite phase and crystallization from the liquid phase, in addition to the diffusional growth based on the diffusion-controlled growth mechanism, as described in Section II-1. The increments in the precipitated and crystallized austenites were calculated from eqs. (16) and (17), respectively. The change in carbon concentration of liquid phase due to cooling by ΔT, $(C_4'-C_4)$ in eq. (17), is always much larger than that of the δ-ferrite phase, (C_1-C_1') in eq. (16), because of the significant difference between the slope of the liquidus line and that of solvus line in the phase diagram (compare the coefficients between eqs. (12) and (15)). Therefore, the increment in the crystallized austenite calculated

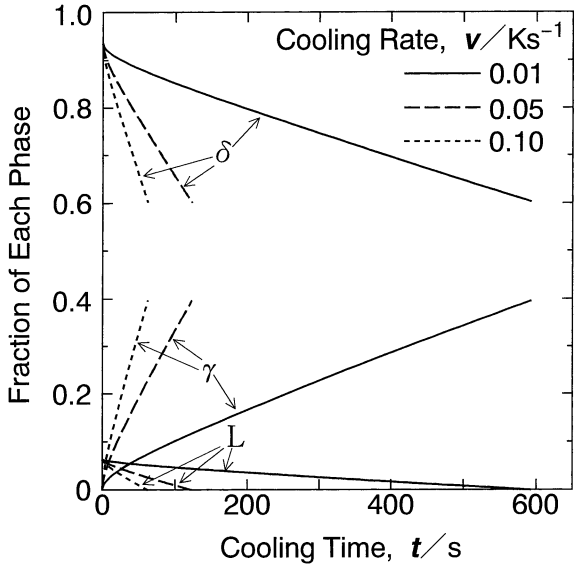

Fig. 4 Change in fractions of δ-ferrite, austenite and liquid phases during cooling of an alloy with 0.12 mass% carbon.

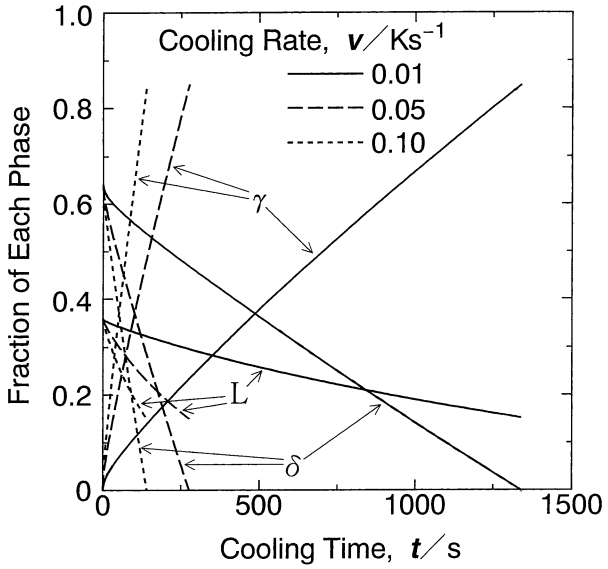

Fig. 6 Change in fractions of δ-ferrite, austenite and liquid phases during cooling of an alloy with 0.25 mass% carbon.

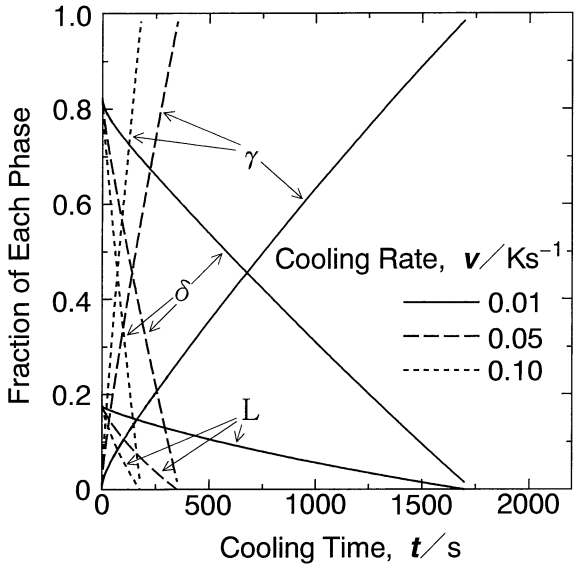

Fig. 5 Change in fractions of δ-ferrite, austenite and liquid phases during cooling of an alloy with 0.17 mass% carbon.

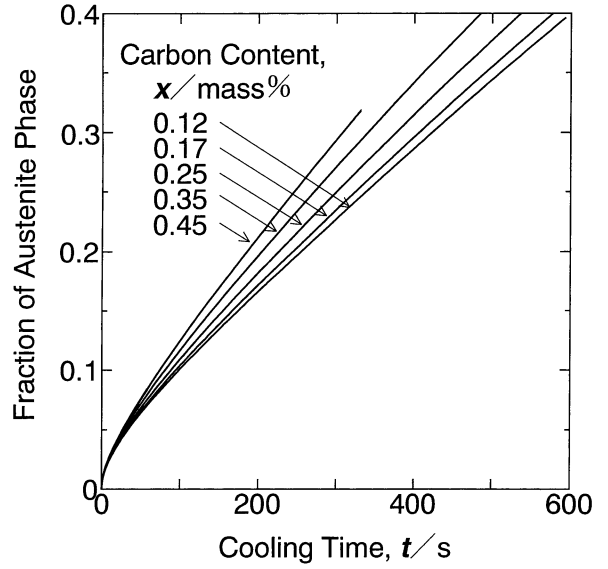

Fig. 7 Effect of carbon content on the growth behavior of austenite phase during the peritectic transformation. Cooling rate is 0.01 K/s.

from eq. (17) is larger than that in precipitated one. According to eq. (17), the increment in the crystallized austenite phase increases with the amount of the liquid phase, x_L, which increases with the carbon content. Consequently, the growth rate of the austenite phase increases with the carbon content.

2. Change in final fraction of each phase with carbon content

Figure 8 shows the effect of carbon content on the fraction of each phase existing after the peritectic transformation. As carbon content increases from 0.09 to 0.17 mass%, the final fraction of the δ-ferrite phase decreases 1 to 0, while that of the austenite phase increases from 0 to 1. As the carbon content increases from 0.17 to 0.53 mass%, the final fraction of austenite phase decreases 1 to 0, while that of the liquid phase increases from 0 to 1. The effect of cooling rate is shown by varying it from 0.01 to 10 K/s. The results for the three different cooling rates are very close to each other, and even the results for a very low cooling rate of 0.01 K/s are far from those for an equilibrium condition. The reason for this will be discussed in Section III-3. The effect of cooling rate is enhanced, when the carbon content is between 0.17 and 0.53 mass%; as the cooling rate increases, the fraction of the austenite phase increases, while that of the liquid phase decreases. In order to consider the reason why the effect of cooling rate is limited to this region of carbon

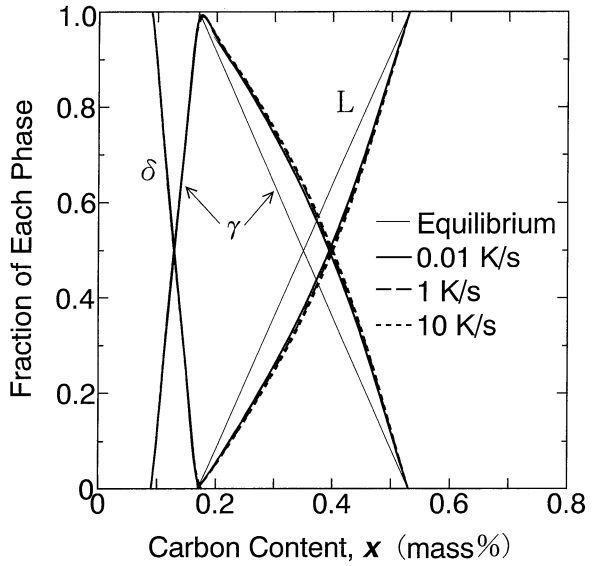

Fig. 8 Effect of carbon content on the fraction of each phase existing after the peritectic transformation.

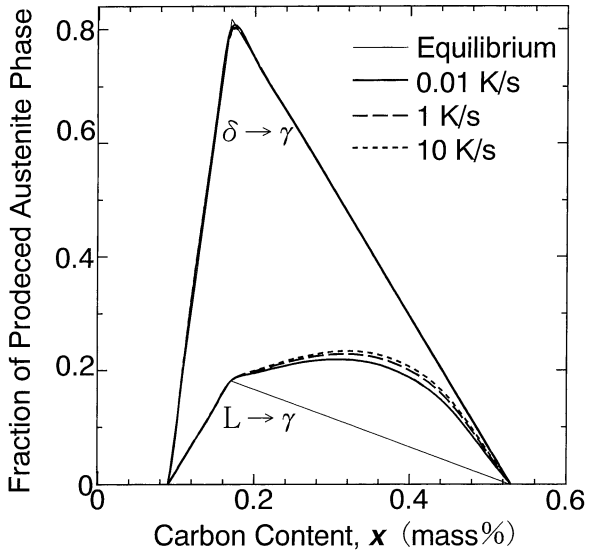

Fig. 9 Effect of cooling rate on the fraction of austenite phase produced by precipitation from the δ-ferrite phase and crystallization from the liquid phase.

contents, we divided the fraction of the austenite phase into that precipitated from the δ-ferrite phase and that crystallized from the liquid phase, by subtracting the final fractions of the phases from the initial ones.

Figure 9 shows the effect of cooling rate on the fraction of austenite produced by precipitation from δ-ferrite and that of austenite produced by crystallization from liquid. As cooling rate increases, the fraction of the crystallized austenite phase increases, when the carbon content is between 0.17 and 0.53 mass%. When the carbon content is between 0.09 and 0.17 mass%, the fraction of the precipitated austenite phase increases with cooling rate, but the increments are very small. The difference in effect of cooling rate between precipitation and crystallization can be explained from the difference in slope between the solvus and liquidus lines, as described in Section III-1.

The amount of the $\delta \rightarrow \gamma$ transformation is shown in Fig. 9. Because the density of austenite is higher than that of δ-ferrite, transformation shrinkage occurs. If the tensile stress caused by this shrinkage exceeds the strength of the solidifying shell, surface cracking can occur. Matsumiya *et al.*[16] pointed out that a key to the consideration of the stress generation is not the total amount of the $\delta \rightarrow \gamma$ transformation but the amount of austenite transformed after the solid fraction reached a high level. Figure 10 shows the effect of solid fraction on the amount of the $\delta \rightarrow \gamma$ transformation, presenting the relationship between the carbon content and the amount of the austenite phase which was transformed after the solid fraction, f_s, had reached the values described in the figure. The total amount of the transformed austenite reaches the maximum at 0.17 mass% carbon. However, as the solid fraction increases, the carbon content corresponding to the peak moves toward the low carbon side; when the solid fraction is 0.90, for example, the peak is between approximately 0.14 and 0.17 mass%, which may be related to the fact that the peak of the

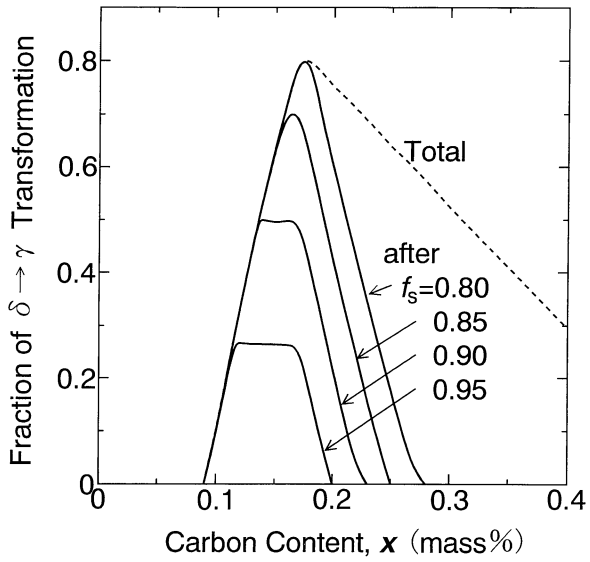

Fig. 10 Relationship between carbon content and the amount of austenite phase transformed after the solid fraction reached high values. Cooling rate is 0.01 K/s.

index on surface cracks is between approximately 0.14 and 0.15 mass% carbon[17].

3. Finishing time and temperature of peritectic transformation

Figure 11 shows the effect of carbon content on the finishing time of the peritectic transformation. The finishing time increases, as the carbon content increases from 0.09 to 0.17 mass%, but it decreases, as carbon content increases further to 0.53 mass%. As shown in Fig. 8, when the carbon content is between 0.09 and 0.17 mass%, some of the δ-ferrite phase remains after the peritectic transformation, while when between 0.17 and 0.53

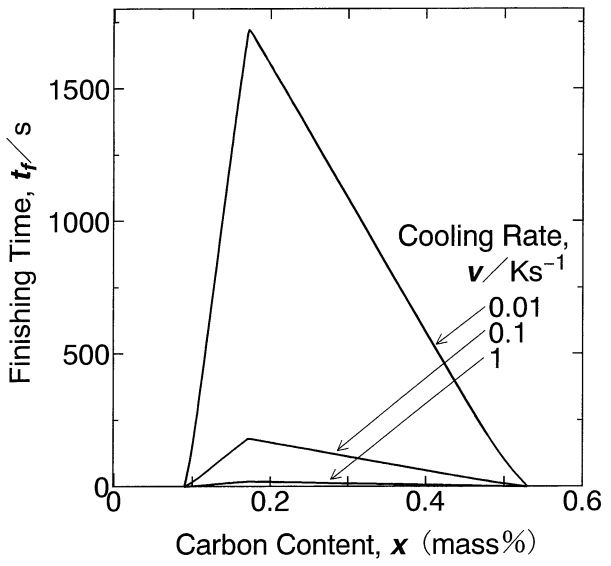

Fig. 11 Effect of carbon content on the finishing time of the peritectic transformation.

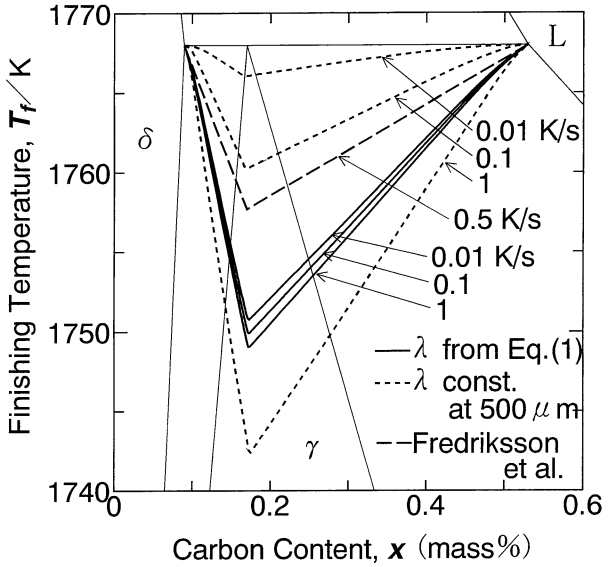

Fig. 12 Effect of carbon content on the finishing temperature of the peritectic transformation. The iron-carbon equilibrium phase diagram is superimposed.

mass%, some of liquid phase remains, but when carbon content is 0.17 mass%, all the reactants of δ-ferrite and liquid phases transform into austenite phase. Therefore, the finishing time reaches the maximum at 0.17 mass% carbon. The increase in cooling rate shortens the finishing time. Because the rapid transformation can cause the generation of stress with a high level, low cooling rates will be preferable from a view point of reducing surface cracks.

Figure 12 shows the effect of carbon content on the finishing temperature of the peritectic transformation. We simulated the process of peritectic transformation during cooling at various cooling rates under a condition of a fixed dendrite arm spacing of 500 μm, which corresponds to a two-step cooling process with a cooling rate of approximately 0.5 K/s above the peritectic temperature and different cooling rates below it, and we compared the results with those calculated under a condition of variable dendrite arm spacing, which decreases from 3374 to 1117 and 370 μm in accordance with eq. (1), when cooling rate increases from 0.01 to 0.1 and 1 K/s. Under an equilibrium condition, the finishing temperature is the peritectic temperature of 1768 K, independent of the carbon content of the alloy. Under a condition of cooling at a finite cooling rate, however, the finishing temperature changes depending on the carbon content; as the carbon content increases, the finishing temperature drops and reaches the minimum at a carbon content of 0.17 mass%, and then it rises toward the peritectic temperature. As the cooling rate increases, the finishing temperature goes down, but the effect of cooling rate is very little. In the results obtained by Chuang *et al.*[6], the effect of local solidification time, which changes with cooling rate, was also very small; when the local solidification time changed from 388 to 1 s, the change in finishing temperature for a carbon content of 0.39 mass% was only 1.8 K. When the dendrite spacing is fixed to 500 μm, the effect of cooling rate is remarkable. As cooling rate decreases, the diffusion time increases, and therefore the finishing temperature comes closer to the equilibrium peritectic temperature. However, when dendrite spacing changes with cooling rate, the diffusion distance also increases with the decrease in cooling rate, and it takes very long time to finish the peritectic transformation. Therefore, the finishing temperature goes down significantly, even when cooling rate is very low.

The result by Fredriksson and Stjerndahl[7] is also shown in Fig. 12. The present results are close to their result, but the finishing temperature in the present results is always lower. The diffusion coefficient of carbon in austenite phase and the concentrations of carbon at the interfaces change with temperature, as described in eqs. (6) and (12) through (15). However, in the calculation by Fredriksson and Stjerndahl, they were taken as constant values. The dendrite arm spacing used in the present calculation is different from that they used. These difference in condition of calculation may have brought about the difference in the results. Takahashi *et al.*[18] investigated the distribution of carbon concentration in an iron-carbon alloy containing 0.29 mass% carbon, and estimated the finishing temperature of the peritectic transformation. According to their report, when the cooling rate was 0.15 K/s, a low concentration of carbon corresponding to that of the δ-ferrite phase was detected in a sample quenched from 1713 K, while when 0.06 K/s, the low concentration was not detected. Their results indicate that the finishing temperature is above 1713 K for a cooling rate of 0.06 K/s and below it for 0.15 K. The finishing temperature estimated from Takahashi's results are strikingly different from ours, but the results of their experiment imply that the finishing temperature of the peritectic transformation during cooling is very low.

IV. Conclusions

The process of peritectic transformation during cooling of iron-carbon alloys was simulated by a numerical analysis, and the effects of carbon content and cooling rate on the growth behavior of austenite phase were investigated. The results are summarized as follows.

The growth of austenite phase during the peritectic transformation proceeds with the precipitation from δ-ferrite phase and the crystallization from liquid phase with the decrease in temperature, in addition to the diffusion of carbon from liquid through austenite to δ-ferrite. The amount of austenite phase produced by the peritectic transformation increases with cooling rate, particularly when carbon content is between 0.17 and 0.53 mass%. The increase in produced austenite is chiefly caused by the crystallization of the austenite phase from the liquid phase. The amount of austenite phase which precipitates from the δ-ferrite phase reaches the maximum at 0.17 mass% carbon. However, the carbon content corresponding to the maximum of the amount of the austenite phase which is produced in a final period of solidification moves toward the low carbon side. The finishing time of the peritectic transformation changes with the total amount of the produced austenite, and it increases with the decrease in cooling rate. Although the finishing temperature is constant at the peritectic temperature of 1768 K under an equilibrium condition, it decreases with the increase in cooling rate under a condition of cooling at a finite rate. The finishing temperature is lowest, when the carbon content is 0.17 mass%.

REFERENCES

(1) T. B. Massalski: *Binary Alloy Phase Diagrams*, Vol. 1, ASM, Materials Park, (1990), p. 842.
(2) T. Matsumiya, T. Saeki, J. Tanaka and T. Ariyoshi: Tetsu-to-Hagané, **68** (1982), 1782.
(3) H. Fredriksson: Scand. J. Metall., **5** (1976), 27.
(4) Y. Itoh, N. Narita and K. Matsubara: Tetsu-to-Hagané, **67** (1981), 755.
(5) S. Mizoguchi: Bulletin Japan Inst. Metals, **26** (1987), 490.
(6) Y. K. Chuang, D. Reinisch and K. Schwerdtfeger: Metall. Trans. A, **6A** (1975), 235.
(7) H. Fredriksson and S. Stjerndahl: Met. Sci., **16** (1982), 575.
(8) M. Enomoto: Tetsu-to-Hagané, **80** (1994), 653.
(9) K. Matsuura, Y. Itoh and T. Narita: ISIJ Int., **33** (1993), 583.
(10) K. Matsuura, H. Maruyama, Y. Itoh, M. Kudoh and K. Ishii: ISIJ Int., **35** (1995), 183.
(11) K. Matsuura, M. Kudoh and T. Ohmi: ISIJ Int., **35** (1995), 624.
(12) K. Matsuura, H. Maruyama, M. Kudoh and Y. Itoh: ISIJ Int., **35** (1995), 1483.
(13) H. D. Brody and M. C. Flemings: Trans. TMS-AIME, **236** (1966), 615.
(14) M. Ibaraki, T. Okamoto and K. Matsumoto: J. Japan Inst. Metals, **32** (1968), 396.
(15) Y. Ueshima, S. Mizoguchi, T. Matsumiya and H. Kajioka: Metall. Trans. B, **17B** (1986), 845.
(16) T. Matsumiya, T. Saeki, J. Tanaka and T. Ariyoshi: Tetsu-to-Hagané, **68** (1982), 1782.
(17) T. Saeki, S. Ooguchi, S. Mizoguchi, T. Yamamoto, H. Misumi and A. Tsuneoka: Tetsu-to-Hagané, **68** (1982), 1773.
(18) T. Takahashi, K. Osasa and J. Tanaka: Tetsu-to-Hagané, **73** (1987), 99.